



Published in final edited form as:

Joint Bone Spine. 2013 December ; 80(6): 613–620. doi:10.1016/j.jbspin.2013.01.001.

Sirt1-deficient mice exhibit an altered cartilage phenotype

Odile Gabay^{a,*}, Kristien J. Zaal^b, Christelle Sanchez^c, Mona Dvir-Ginzberg^d, Viktoria Gagarina^a, Yingjie Song^e, Xiao Hong He^f, and Michael W. McBurney^f

^a Cartilage Biology and Orthopedic Branch, National Institute of Arthritis and Musculoskeletal and Skin Diseases, National Institutes of Health, 50 South Drive, Bethesda, MD, USA

^b Light Imaging Section, Office of Science & Technology, National Institute of Arthritis and Musculoskeletal and Skin Diseases, National Institutes of Health, Bethesda, MD, USA

^c Bone and Cartilage Research Unit, Institute of Pathology B23, University of Liege, Liege, Belgium

^d Laboratory of Cartilage Biology, Institute of Dental Sciences, Faculty of Dental Medicine, Hebrew University-Hadassah Ein Kerem, Jerusalem, Israel

^e Uniformed Services University of the Health Sciences, Department of Surgery, Bethesda, MD, USA

^f Cancer Therapeutics, Ottawa Hospital Research Institute, 501 Smyth Road, Box 926, Ottawa, Ontario, Canada, K1H 8L6

Abstract

Objective—We previously demonstrated that Sirt1 regulates apoptosis in cartilage *in vitro*. Here we attempt to examine *in vivo* cartilage homeostasis, using Sirt1 total body knockout (KO) mice.

Method—Articular cartilage was harvested from hind paws of 1-week and 3-week-old mice carrying wild type (WT) or null Sirt1 gene. Knees of Sirt1 haploinsufficient mice also were examined, at 6 months. Joint cartilage was processed for histologic examination or biochemical analyses of chondrocyte cultures.

Results—We found that articular cartilage tissue sections from Sirt1 KO mice up to 3 weeks of age exhibited low levels of type 2 collagen, aggrecan, and glycosaminoglycan content. In contrast, protein levels of MMP-13 were elevated in the Sirt1 KO mice, leading to a potential increase of cartilage breakdown, already shown in the heterozygous mice. Additional results showed elevated chondrocyte apoptosis in Sirt1 KO mice, as compared to WT controls. In addition to these observations, PTP1b (protein tyrosine phosphatase b) was elevated in the Sirt1 KO mice, in line with previous reports.

Conclusion—The findings from this animal model demonstrated that Sirt1 KO mice presented an altered cartilage phenotype, with an elevated apoptotic process and a potential degradative cartilage process.

Keywords

Sirtuin 1; Cartilage; Osteoarthritis; Animal models

1. Introduction

Osteoarthritis (OA) is a complex and multifactorial degenerative disease, leading to an imbalance between the catabolic and anabolic factors in cartilage. Different mechanisms are involved, such as inflammation, apoptosis, and breakdown of major extra-cellular matrix components, such as aggrecan and, type 2 collagen under the control of matrix metalloproteases, (MMPs), such as aggrecanases and collagenases [1]. It has been well documented that aging is a key risk factor in OA susceptibility [2,3]. In fact, more than 50% of adults aged 65 or more reported an arthritis diagnosis, making OA one of the most common diseases in developed countries [4].

Sirt1 has been shown to regulate lifespan and aging in simple eukaryotes and in rodents [2,5,6]. In mammals, Sirt1 has been reported to play an important role in age-related diseases such as osteoporosis, diabetes, and cancer [6–8]. Similarly, we have previously shown *in vitro* that Sirt1 modulates gene expression in human osteoarthritic chondrocytes. Sirt1 positively regulates the expression of extracellular matrix (ECM)-encoding genes of cartilage [9]. Further, Sirt1 enhances survival of human OA chondrocytes by repressing apoptosis [10,11]. Recently, Sirt1 has been reported to be involved in the pathogenesis of OA by modulating chondrocyte gene expression and hypertrophy [12]. Finally, Sirt1 plays an anti-inflammatory role in different tissues by inhibiting the transcription of pro-inflammatory-responsive genes [6].

Despite the growing evidence supporting *in vitro* studies demonstrating Sirt1's protective role in cartilage, few studies have established that these roles also exist *in vivo*. We created Sirt1-null mice [13,14] and found that – compared with normal mice – they were smaller, had cranio-facial abnormalities, and their long bones mineralized slower [15]. These observations were consistent with the notion that Sirt1 may play a role in cartilage development and homeostasis. Additional observations of heterozygous Sirt1 mice (Sirt1^{+/-}) showed that they exhibit increased apoptotic chondrocytes and OA severity with age, as compared to equivalent WT mice [16].

In this study, we investigated articular cartilage of mice lacking the Sirt1 protein (KO mice) and report that they were predisposed to develop OA because they present characteristic features of articular cartilage degeneration, even at a young age. Our results showed an altered cartilage phenotype in these mice due to a higher level of cartilage breakdown and apoptosis in the Sirt1-deficient mice.

2. Methods

2.1. Animals

Experiments were performed on Sirt1-deleted 129/J mice aged 2 days, 7 days, and 3 weeks. Sirt1 knockout mice are indicated as KO (total $n = 9$), and wild-type as WT (total $n = 20$). Littermates were generated from matings between the Sirt1^{+/-} animals. In complement, Sirt1^{+/-} animals were also examined at 6 months for histopathology and scored by the OA OARSI grading. Genomic DNA from mice tail fragments was used for genotyping using the Extract-N-Amp Tissue PCR kit (Sigma, St Louis, MI). PCR primer sequences designed to amplify the native Sirt1 and the deleted Sirt1 were (Forward) 5'-TTCACATTGCATGTGTGTGTG-3' for both and (Reverse) 5'-TAGCCTGCGTAGTGTGGTG-3', and 5'-ATTTGGTAGGGACCCAAAGG-3', respectively. All animals were housed at Taconic, Maryland, under standard conditions of temperature, light, food and water. All procedures were performed in accordance with NIH Committees for Animal Use and Care (ARAC) guidelines.

2.2. Primary mouse cell culture, cell count, and flow cytometry

Isolation of costal cartilage from KO, or WT 7-day-old mice, and chondrocytes plating were adapted from Gabay et al. [17]. Briefly, pieces of costal cartilage were incubated in collagenase 3 mg/mL for 1 h 30 min at 37 °C, carefully isolated from soft tissue in PBS, incubated in collagenase 0.5 mg/mL overnight. Chondrocytes were washed, centrifuged and plated for a 7–10 day period wherein they were allowed to propagate. Passages 0 and 1 chondrocytes were used for experiments because cartilage marker genes maintained expression. Monolayer cultures were maintained in culture conditions, as previously described [17], and growth medium was replaced every 3 days. Prior to analysis, cells were rinsed with PBS, trypsinized with Trypsin 0.25%, resuspended in 10 ml of growth medium, and counted with a hemocytometer using trypan blue exclusion assay.

For analyses of cell death via flow cytometry, the cells were rinsed once in chilled PBS, trypsinized, then resuspended in 10 ml of Dulbecco's modified Eagle's medium supplemented with 10% fetal bovine serum. The cells were pelleted and resuspended in 100% methanol. Cells were kept on ice for 10 min, pelleted, and treated with RNase A (180 µg; Sigma, St Louis, MI) for 30 min at room temperature. Propidium iodide (Sigma, St Louis, MI) was added to a final concentration of 75 mg/ml. Cell cycle analysis was performed on a Coulter Profile 2 flow cytometer.

2.3. Protein extraction and immunoblotting

Whole-cell protein extracts were carried out according to Dvir-Ginzberg et al., 2008 [9]. The protein extracts were resolved by sodium dodecyl sulfate–polyacrylamide gel electrophoresis (10 µg protein/lane) and transferred onto PVDF membranes for immunoblotting. The blots were processed as previously described and probed with antibodies. Blots were developed using an alkaline phosphatase-conjugated secondary antibody and developed with BCIP/nitroblue tetrazolium solution (Invitrogen, Camarillo, CA). Antibodies were purchased from Abcam (Cambridge, MA) for PTP1b, MMP-13 and beta-actin, and Upstate/Millipore (Temecula, CA) for Sirt1.

2.4. Histology and immunohistochemistry

For immunohistochemical analysis, cartilage samples were fixed in 4% paraformaldehyde for 24 to 48 hours, dehydrated in a graded series of ethanol baths, embedded in paraffin, and cut into 5- μ m sections. Slides were rehydrated and incubated with mouse anti-Aggregan, mouse-anti-Type II Collagen (Millipore, Temecula, CA), mouse-anti-PTP1b (Abcam, Cambridge, MA), or mouse anti-matrix metalloprotease- (anti-MMP-13,-1,-3,ADAMTS-4,ADAMTS-5) Abcam, Cambridge, MA) specific antibodies and visualized using a broad-spectrum immunohistochemistry kit (DAB, diaminobenzidine, Invitrogen, Camarillo, CA).

To test the presence of glycosaminoglycans, sections were stained with alcian blue and with safranin-O/light green to examine subchondral bone and OA. Joints of the paws and the knees were examined for 1 week and 3 week-old mice.

Cartilage defects at 6 months in the +/- were assessed in accordance with the OsteoArthritis Research Society International (OARSI) histopathology initiative-recommendations for histological assessment of OA in mice [18].

Total skeletal coloration was performed with basic ethanol-KOH:glycerol alizarin red-alcian blue, according to Depew [19]. Results were analyzed using the Color Atlas of Fetal Skeleton of the mouse, rat and rabbit [20].

2.5. Statistical analysis

Means and standard deviations were calculated. Statistical analysis was performed using one-way analysis of variance, assuming confidence levels of 95% ($P < 0.05$) to be statistically significant. Error bars represent the standard deviation around the mean value of each data point. An asterisk (*) was used to denote statistically significant differences between controls and experimental conditions. The immunoblots represent two repetitions of three different experiments ($n = 6$). For IHC, the mean of positive stain cells was determined; stained cells reflected a greater than 10-fold intensity above the background, determined by scanning densitometry (Image J software). A scoring method adapted from Lee et al., [21] was used well to determine the coloration of the tissue matrix. An average of three fields from three sections of each separate geno-type (-/-, +/+) of three different animals were assessed. Each field was blindly read by two different readers. Cartilage defects were scored in accordance with the OARSI histopathology initiative OA scoring for mice [18].

3. Results

3.1. Sirt1 KO mice exhibited defects in the cartilage of the skull, spine, rib cages, and joints, consistent with their reduced size

Examination of the two strains shows a reduced size for the Sirt1 KO mice, as compared to the wild types, at 2, 7 days and 3 weeks. Some exterior defects are also evident, such as closed eyes and bad fur at 1 week (Fig. 1). At 2 days, the mice already exhibit a difference in size (Fig. 1B). Skeletal staining at 2 days on the Sirt-1 KO and Sirt1 Wild type mice (Fig.

1C), confirmed that Sirt1 KO mice exhibit a smaller size, cranio-facial and eye defects compared to their littermate, in line with previous reports [13,15].

We further examined the effect on the skeleton and cartilage on the same mice (Fig. 2). Sirt1 KO mice exhibited less cartilage in the skull, rib cage, spine and in knee joints, due to their size. They all exhibited less bone mineralization which implies defects in cartilage hypertrophy attributing to delayed skeletal development. Interestingly, the sutures of the calvariae were not fixed in the KO, compared with the WT mice (arrows). These observations were similar in all KO analyzed, as compared with the WT mates ($n = 3$ each).

3.2. Articular cartilage tissue from Sirt1 KO exhibited low levels of type 2 Collagen, Aggrecan and Glycosaminoglycan (GAG) content in the paws, and a high level of MMP-13

The superficial zone from articular cartilage of distal interphalangeal joints of the posterior paws, were examined. Alcian blue coloration was carried out to visualize glycosaminoglycan (GAG) content, which are hallmarks of healthy cartilage. Results, illustrated in Fig. 3, showed less GAG content in KO paws as compared to WT. To further assess levels of aggrecan and type 2 Collagen, immunohistochemistry for cartilage was carried out and quantified using densitometry and statistical analysis. Overall, the paws showed a decrease in alcian blue intensity, aggrecan, and type 2 collagen in the KO (60%, 52%, and 21%, respectively) as compared to WT mice at 1 week of age.

To determine whether the catalytic enzymes involved in cartilage degeneration were elevated in the KO mice, we performed immunohistochemistry for matrix metalloproteinase (MMP) –13, aggrecanase, which have been documented to be elevated in OA [22]. As shown in Fig. 4, this MMP is increased in the cartilage of the KO mice, compared with their littermates. Immunostaining for MMP-1, MMP-3, ADAMTS-4, and –5 was similar between KO and WT at 3 weeks of age (data not shown).

Because KnockOut mice die in early age, additional analyses and scoring were carried out in accordance with the OARSI initiative OA scoring for adult mice in the heterozygous mice (Fig. 5) The Sirt1^{+/-} mice presented elevated cartilage degeneration at 6 months, with a total mean score of 3.9, corresponding to moderate OA relative to their WT littermates which possessed a score of 1.25 corresponding to early-stage OA.

3.3. Enhanced apoptosis in cartilage of Sirt1 KO compared to WT mice; PTP1b is elevated in Sirt1 KO mice cartilage compared with WT mice

Mice chondrocytes from each genotype were cultured and counted daily. Whereas WT chondrocytes grew normally, articular chondrocytes derived from the Sirt1 KO mice did not propagate in culture (Fig. 6A). FACS analyses indicated elevated numbers of apoptotic cells in cultures of KO chondrocytes at 2 and 4 days (Fig. 6B). This data supports that Sirt1 contributes to chondrocyte proliferation and lack of it could lead to limited growth and development of cartilage.

As previously published by Gagarina et al. in 2010, Sirt1 may prevent chondrocyte apoptosis in a protein tyrosine phosphatase b (PTP1b)-dependent manner. To examine PTP1b expression *in vivo*, immunoblot analyses were carried out. Immunoblot analyses of

proteins derived from the different genotypes confirmed that PTP1b was elevated in Sirt1 KO mice compared with WT controls (Fig. 6C), further supporting the enhanced levels of apoptotic chondrocytes in KO mice.

4. Discussion

Recent publications show that the protein deacetylase Sirt1 plays an important role in cartilage biology and homeostasis [9,10,15,23,24]. Our current study demonstrates that mice lacking Sirt1 protein possess an altered cartilage phenotype, in line with our previous reports in 9 month Sirt1 haploinsufficient mice [16]. Further, we describe two different phenomena underlying this phenotype: an increase in chondrocyte apoptosis and an accelerated articular cartilage breakdown showing a regulation of cartilage by Sirt1 *in vivo*.

The Sirt1-null mice were smaller in size compared to WT mice in equivalent ages, which agrees with previous reports [13,14,25]. We also found obvious defects on the skin that could benefit further investigation. These mice suffer high perinatal mortality, particularly when carried on an inbred mouse strain. Indeed, *in vitro* analyses showed that chondrocytes isolated from pups surviving 7 days after birth, did not attach properly, frequently apoptosed, and were found floating in culture growth media. Here we conclude that much of the age-related cartilage phenotype is attributed to Sirt1 protein.

We also compared histologic data for the WT and Sirt1 heterozygous strains at 6 months presented Fig. 5, because the KO mice were not alive at this age. As seen in the pictures, heterozygous mice possess a significant enhancement in OA severity and cartilage degradation as compared to WT mice at 6 months.

We previously showed that Sirt1 enhances the survival of human osteoarthritic chondrocytes by repressing protein tyrosine phosphatase 1b and activating the insulin-like growth factor receptor pathway [10,15]. Consistent reports show that using Sirtuin inhibitors for Sirt1 and Sirt2 induced cell death through p53 hyper-acetylated [26]. Accordingly, and in line with our current report, altering Sirt1 levels could lead to enhanced cell death via multiple mechanisms and diminish the protective effect Sirt1 holds on chondrocyte viability *in vivo*.

Very few studies have demonstrated the role of Sirt1 *in vivo* with regards to cartilage biology or age-induced arthritis. As mentioned, our recent publication comparing WT and haploinsufficient Sirt1 mice compared musculoskeletal features, OA severity scoring, and apoptosis in cartilage of 1-month-old and 9-month-old mice [16]. The results showed a significant decrease in Sirt1 protein levels in the heterozygous mice compared with their littermates at 1 month. Interestingly, both strains ceased to express full-length Sirt1 at 9 months.

Sirt1 KO mice showed an accelerated cartilage degenerative process and early onset OA features. Accumulation of matrix metalloproteinases in the cartilage and low levels of type 2 collagen and aggrecan could predict very weak mechanical properties of cartilage in these mice, making them susceptible to cartilage degeneration. Our study showed increased MMP-13, aggrecanase, with reduced ECM content in the KO mice at 3 weeks of age. However, it is not yet clear if the decreased intensity of aggrecan, type 2 collagen and GAG

content in our experiments is due to the decrease of the cellularity within cartilage tissues of KO mice. These data suggest early OA onset exists in KO mice. While MMP-13 levels are elevated in Sirt1 KO mice, other aggrecanases did show a similar increase in these mice strains. It appears that collagen type 2 breakdown and MMP-13 were most affected and correlated well with OA severity in Sirt1 *in vivo* mice model used herein.

The present communication further accentuates that Sirt1 is necessary for the normal development of articular cartilage *in vivo*. In its absence, even at a young age, mice develop cartilage degeneration and early-onset OA, which is normally developed with advanced age.

Acknowledgements

Authors acknowledge, Drs: Yongqing Chen for the mice pictures, Jeff Lay for assistance in flow cytometry, Dr Vittorio Sartorelli critically reviewing the manuscript, Evelyne Ralston for providing from imaging platforms. The authors also acknowledge Dr David Engel for editing the manuscript and Mr. Richard Booth for assistance in statistical analyses.

This research was supported by the Intramural Research Program of the National Institutes of Arthritis and Musculoskeletal and Skin Diseases of the National Institutes of Health.

References

1. Goldring MB. The role of cytokines as inflammatory mediators in osteoarthritis: lessons from animal models. *Connect Tissue Res.* 1999; 40:1–11. [PubMed: 10770646]
2. Zhang WG, Bai XJ, Chen XM. SIRT1 variants are associated with aging in a healthy Han Chinese population. *Clin Chim Acta.* 2010; 411:1679–83. [PubMed: 20633545]
3. Loeser RF. Age-related changes in the musculoskeletal system and the development of osteoarthritis. *Clin Geriatr Med.* 2010; 26:371–86. [PubMed: 20699160]
4. Lawrence RC, Felson DT, Helmick CG, et al. Estimates of the prevalence of arthritis and other rheumatic conditions in the United States. Part II. *Arthritis Rheum.* 2008; 58:26–35. [PubMed: 18163497]
5. Tissenbaum HA, Guarente L. Increased dosage of a sir-2 gene extends lifespan in *Caenorhabditis elegans*. *Nature.* 2001; 410:227–30. [PubMed: 11242085]
6. Michan S, Sinclair D. Sirtuins in mammals: insights into their biological function. *Biochem J.* 2007; 404:1–13. [PubMed: 17447894]
7. Backesjo CM, Li Y, Lindgren U, et al. Activation of Sirt1 decreases adipocyte formation during osteoblast differentiation of mesenchymal stem cells. *J Bone Miner Res.* 2006; 21:993–1002. [PubMed: 16813520]
8. Zeng L, Chen R, Liang F, et al. Silent information regulator, Sirtuin 1, and age-related diseases. *Geriatr Gerontol Int.* 2009; 9:7–15. [PubMed: 19260974]
9. Dvir-Ginzberg M, Gagarina V, Lee EJ, et al. Regulation of cartilage-specific gene expression in human chondrocytes by Sirt1 and nicotinamide phosphoribosyltransferase. *J Biol Chem.* 2008; 283:36300–10. [PubMed: 18957417]
10. Gagarina V, Gabay O, Dvir-Ginzberg M, et al. Sirt1 enhances survival of human osteoarthritic chondrocytes by repressing protein tyrosine phosphatase 1B and activating the insulin-like growth factor receptor pathway. *Arthritis Rheum.* 2010; 62:1383–92. [PubMed: 20131294]
11. Takayama K, Ishida K, Matsushita T, et al. SIRT1 regulation of apoptosis of human chondrocytes. *Arthritis Rheum.* 2009; 60:2731–40. [PubMed: 19714620]
12. Fujita N, Matsushita T, Ishida K, et al. Potential involvement of SIRT1 in the pathogenesis of osteoarthritis through the modulation of chondrocyte gene expressions. *J Orthop Res.* 2011; 29:511–5. [PubMed: 21337390]
13. McBurney MW, Yang X, Jardine K, et al. The mammalian SIR2alpha protein has a role in embryogenesis and gametogenesis. *Mol Cell Biol.* 2003; 23:38–54. [PubMed: 12482959]

14. McBurney MW, Yang X, Jardine K, et al. The absence of SIR2alpha protein has no effect on global gene silencing in mouse embryonic stem cells. *Mol Cancer Res.* 2003; 1:402–9. [PubMed: 12651913]
15. Lemieux ME, Yang X, Jardine K, et al. The Sirt1 deacetylase modulates the insulin-like growth factor signaling pathway in mammals. *Mech Ageing Dev.* 2005; 126:1097–105. [PubMed: 15964060]
16. Gabay O, Oppenheimer H, Meir H, et al. Increased apoptotic chondrocytes in articular cartilage from adult heterozygous SirT1 mice. *Ann Rheum Dis.* 2012; 71:613–6. [PubMed: 22258484]
17. Gabay O, Gosset M, Levy A, et al. Stress-induced signaling pathways in hyalin chondrocytes: inhibition by Avocado-Soybean Unsaponifiables (ASU). *Osteoarthritis Cartilage.* 2008; 16:373–84. [PubMed: 17707661]
18. Glasson SS, Chambers MG, Van Den Berg WB, et al. The OARSI histopathology initiative – recommendations for histological assessments of osteoarthritis in the mouse. *Osteoarthritis Cartilage.* 2010; 18:S17–23. [PubMed: 20864019]
19. Depew MJ. Analysis of skeletal ontogenesis through differential staining of bone and cartilage. *Methods Mol Biol.* 2008; 461:37–45. [PubMed: 19030790]
20. Yasuda M, Yuki T, Tanimura T. Color atlas of fetal skeleton of the mouse, rat, and rabbit. *Congenit Anom.* 1996; 36:263–5.
21. Lee JH, Fitzgerald JB, DiMicco MA, et al. Co-culture of mechanically injured cartilage with joint capsule tissue alters chondrocyte expression patterns and increases ADAMTS5 production. *Arch Biochem Biophys.* 2009; 489:118–26. [PubMed: 19607802]
22. Verma P, Dalal K. ADAMTS-4 and ADAMTS-5: key enzymes in osteoarthritis. *J Cell Biochem.* 2011; 112:3507–14. [PubMed: 21815191]
23. Dvir-Ginzberg M, Gagarina V, Lee EJ, et al. Tumor necrosis factor alpha-mediated cleavage and inactivation of SirT1 in human osteoarthritic chondrocytes. *Arthritis Rheum.* 2011; 63:2363–73. [PubMed: 21305533]
24. Oppenheimer H, Gabay O, Meir H, et al. 75 kDa SirT1 blocks TNFalpha-mediated apoptosis in human osteoarthritic chondrocytes. *Arthritis Rheum.* 2012; 64:718–28. [PubMed: 21987377]
25. Cheng HL, Mostoslavsky R, Saito S, et al. Developmental defects and p53 hyper-acetylation in Sir2 homolog (SIRT1)-deficient mice. *Proc Natl Acad Sci U S A.* 2003; 100:10794–9. [PubMed: 12960381]
26. Peck B, Chen CY, Ho KK, et al. SIRT inhibitors induce cell death and p53 acetylation through targeting both SIRT1 and SIRT2. *Mol Cancer Ther.* 2010; 9:844–55. [PubMed: 20371709]

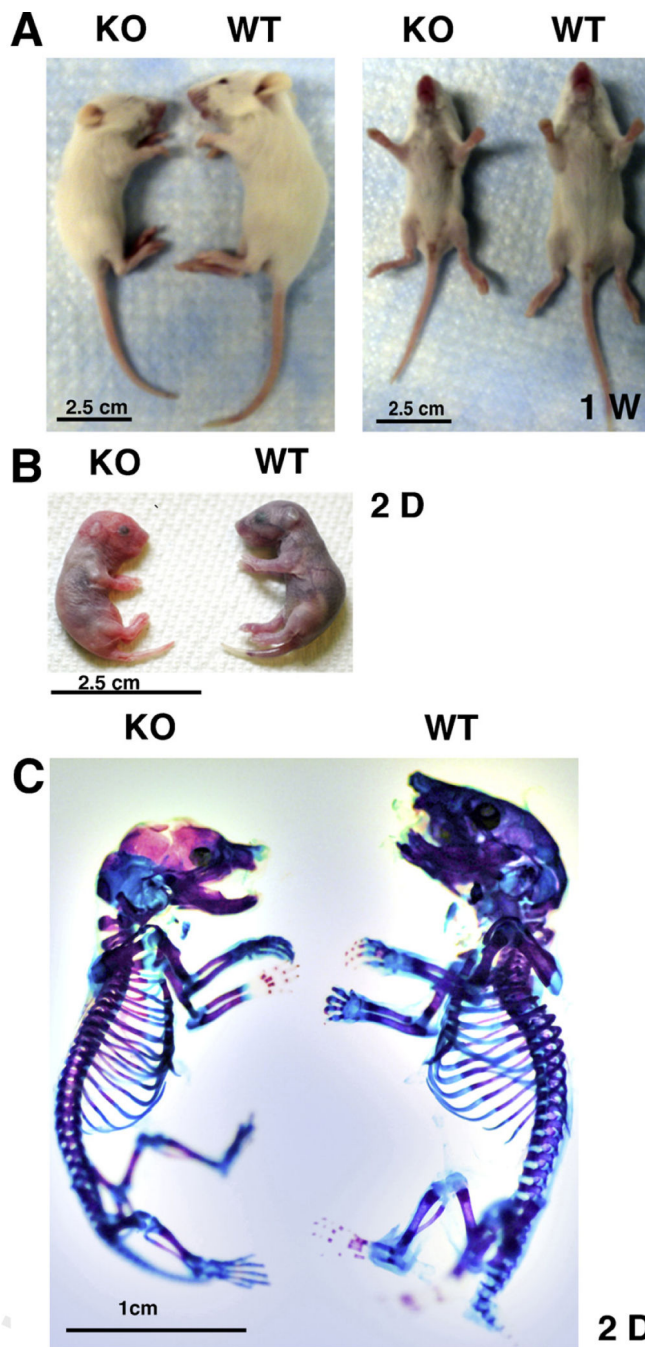


Fig. 1. Cartilage phenotype of Sirt1 KO mice. A. Sirt1 KO on the 129/J background mice. Photograph shows a KO mouse of approximately 2/3 normal size at 1 weeks of age, with closed eyes, obstructed fur and smaller joints compared to the WT. B. At 2 days, before skeletal staining, the Sirt1 KO has already a smaller size. C. Skeletal staining with alizarin red/alcian blue shows disparities in cartilage on the skull, on the rib cage, at the spine and on the big joints.

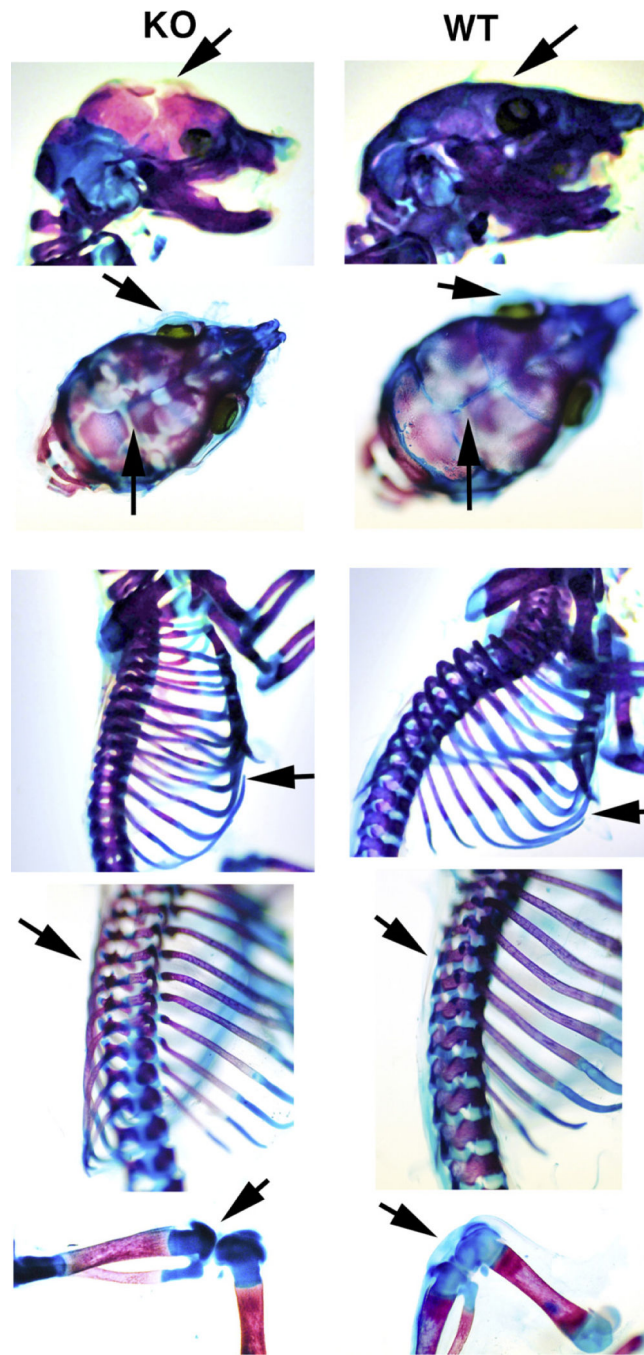


Fig. 2. Skeletal staining with alizarin red/alcian blue, details: the arrows show a reduction in cartilage volume in the KO at each location, and a complete absence of cartilage on the calvariae. The skeletal staining shows a disorganization of the rib cages, a strong eye and joints cartilage defects.

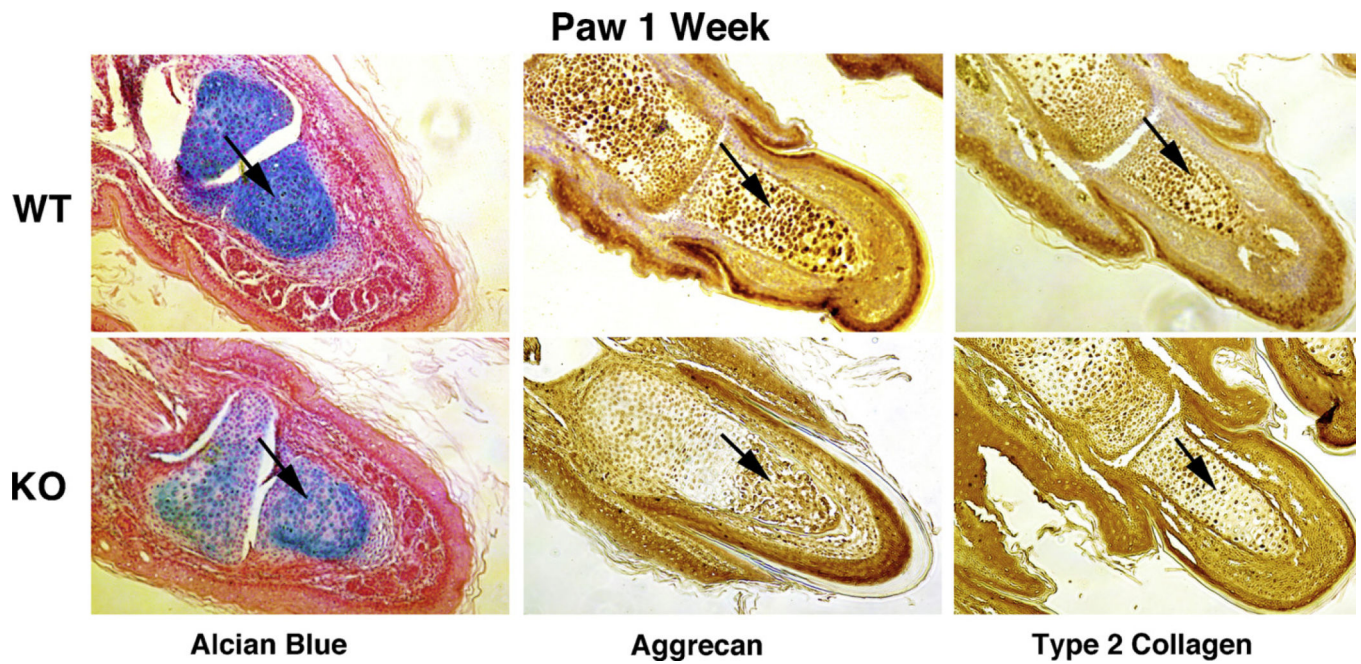


Fig. 3. Articular cartilage from Sirt1 KO shows less aggrecan, type 2 collagen and glycosaminoglycan content than their WT littermates. The paws from each genotype were processed for immunohistochemistry for either aggrecan, type 2 collagen, or alcian blue staining at 1 week. As shown in Fig. 3, alcian blue, aggrecan and type 2 collagen staining intensity were abrogated in the Sirt1 KO at 1 week of age by 60%, 52% and 21% respectively (magnification $\times 10$).

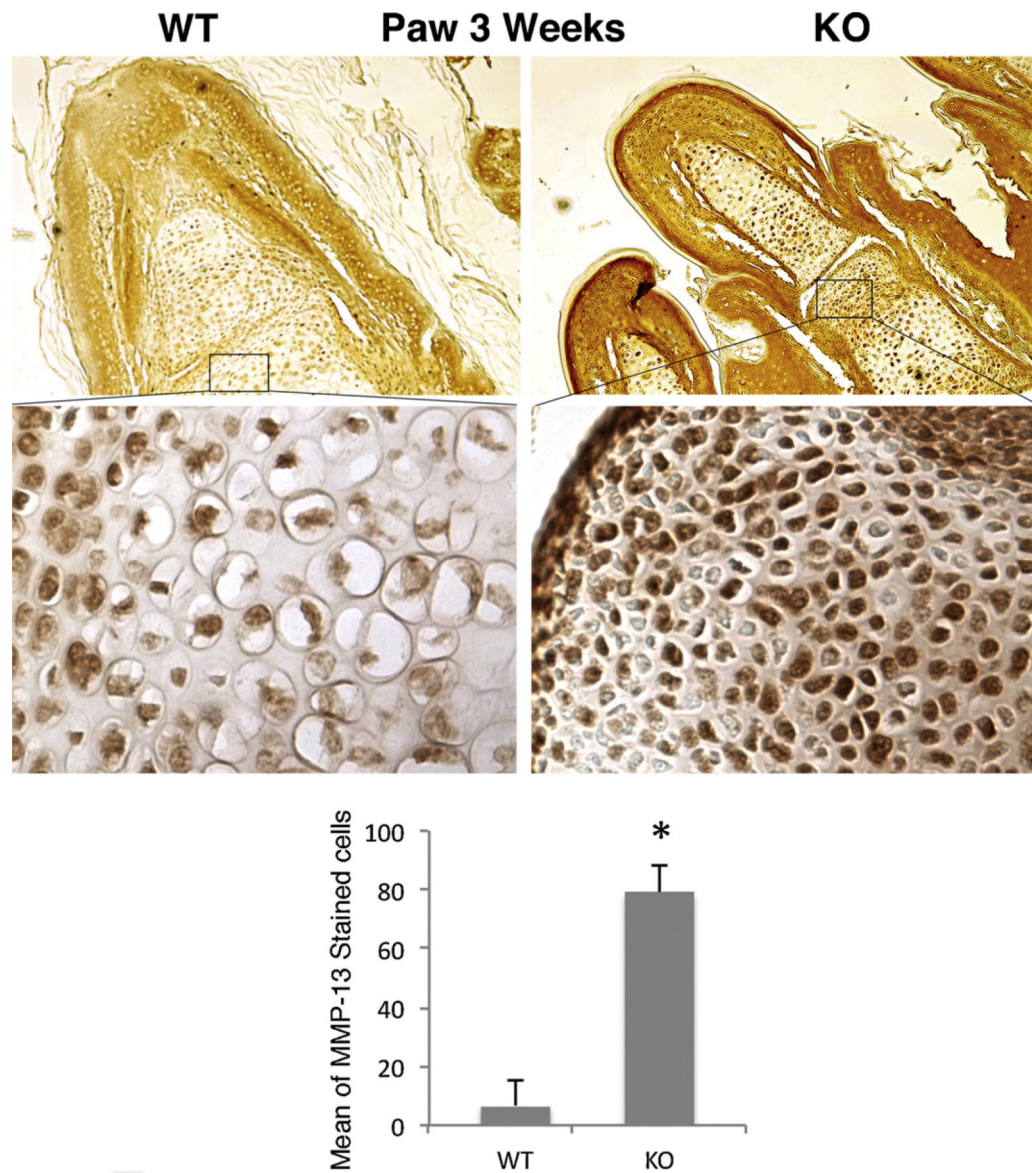


Fig. 4. Elevated protein levels of MMP-13 in Sirt1 KO cartilage at 3 weeks. The paws of 3-week-old mice were processed for immunohistochemistry for MMP-13, and counterstained with hematoxylin ($\times 10$ upper panel and $\times 20$ lower panel). The percent positively stained cells per field were determined for an average of six fields from three sections of three separate mice of each genotype (graph below immunosections). The error bars in all graphs indicate the standard deviation and the statistical significance is indicated by an asterisk, *. $P < 0.001$ ($=1.7189E-5$).

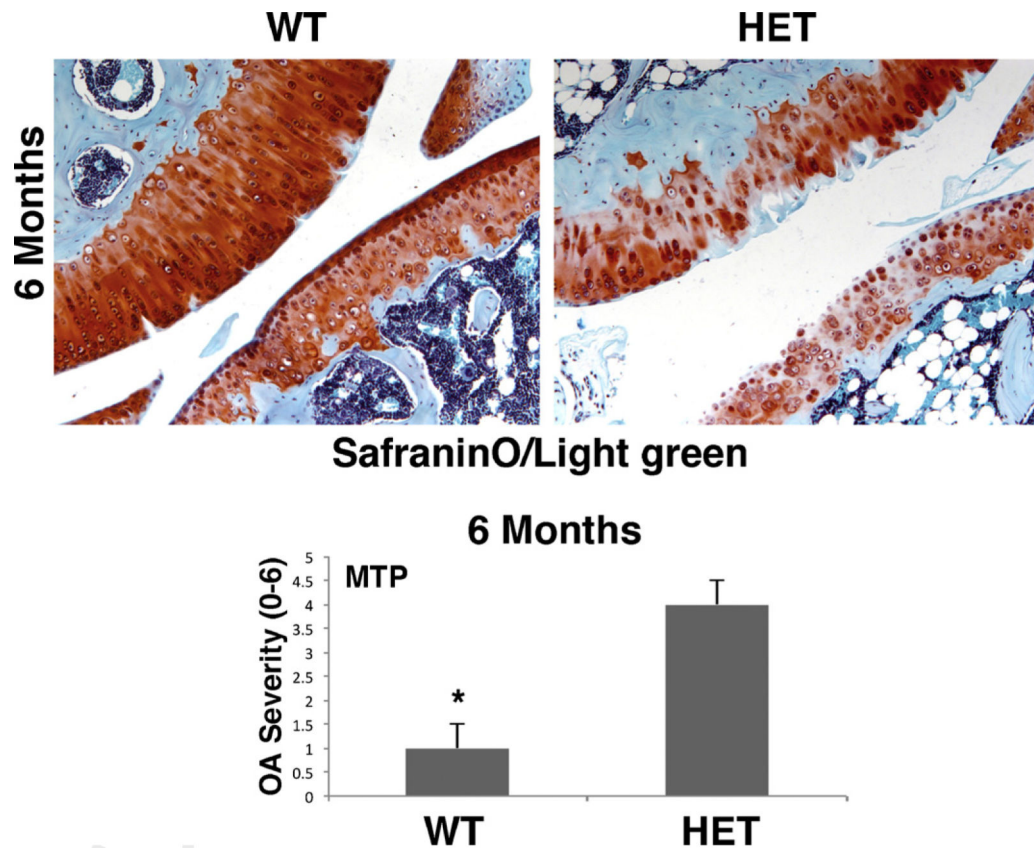


Fig. 5. Elevated cartilage breakdown in older Sirt1 heterozygous mice. Knee sections of 6-month-old WT and Sirt1 heterozygous mice were processed for coloration with safranin-O/Light green. Examination of 36 sections from 6 months mice knees showed significant higher cartilage degradation in the Sirt1 heterozygous as compared with their littermates (magnification $\times 16$). The pictures are representative of the whole analysis. At 6 months, the mean of the cartilage degradation grade, adapted from the OARSI semi-quantitative scoring for OA severity (here, grade 0 = no degradation, grade 5 = denuded cartilage surface with sclerotic bone) showed 3.9 for the Sirt1 heterozygous and 1.2 for the WT ($P < 0.001$). The scoring of 12 samples for each genotype (two sections of two different knees from three different mice from each genotype) showed more severe grades for the Sirt1 heterozygous knees.

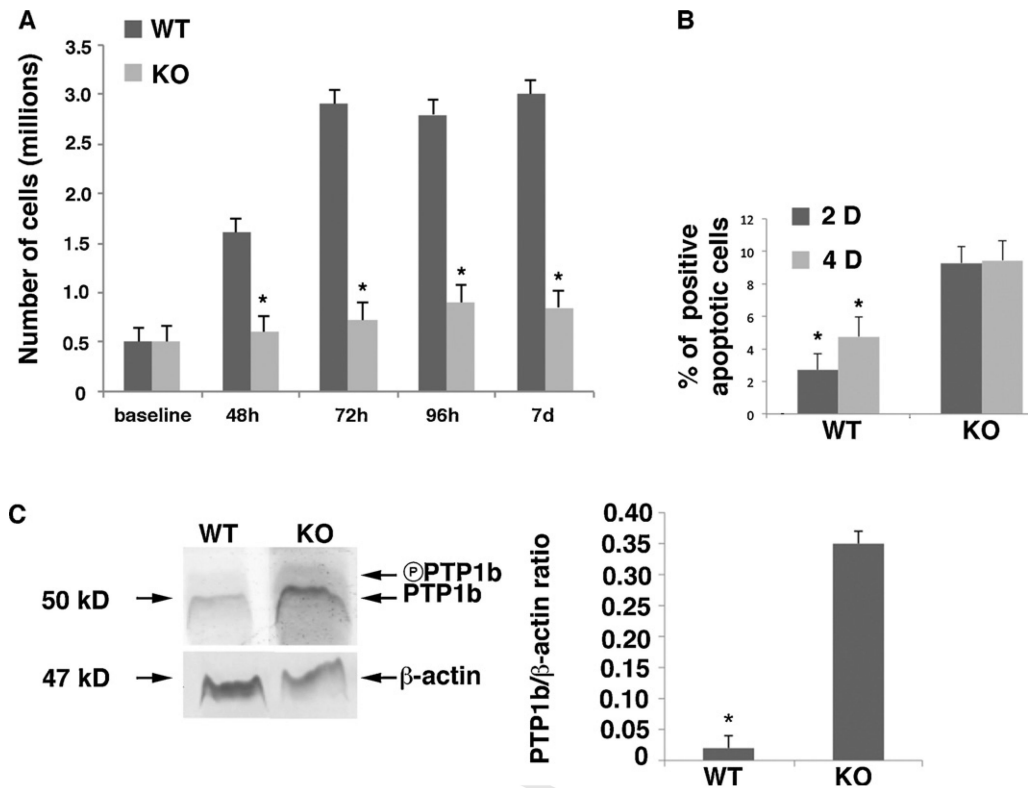


Fig. 6. Increased apoptotic process in Sirt1 KO vs. WT. A. Two different genotypes chondrocytes were plated at 500,000 cells/plate. Student T-test compared the WT and KO (48 h: $P = 5.285 \text{ E-}09$, $P < 0.0001$; 72 h: $P = 6.122 \text{ E-}07$, $P < 0.0001$; 96 h: $P = 3.0066 \text{ E-}07$, $P < 0.0001$; 7 days: $P = 2.5 \text{ E-}05$, $P < 0.0001$ respectively). B. Flow cytometry was carried out for apoptotic cells using the propidium iodide method. The graph represents the apoptotic cells percentage found after 48 h or 4 days of culture. WT and KO exhibited significant differences at 48 h and 4D ($P = 8.08 \text{ E-}06$, $P < 0.0001$ et $P = 6.99 \text{ E-}05$, $P < 0.0001$ respectively). C. Protein extracts from KO and WT genotypes were immunoblotted for PTP1b antibody. The graph represents the ratio PTP1b/beta-actin, by image J scanning densitometry ($P < 0.001$). The error bars in all graphs indicate the standard deviation, and the statistical significance as indicated by an asterisk, *.